

Seismic behaviour of concrete columns with high-strength stirrups

Peng Wang^{*1,2,3}, Qingxuan Shi^{1,2,3a}, Feng Wang^{2b} and Qiuwei Wang^{1,2,3c}

¹State Key Laboratory of Green Building in Western China, Xi'an University of Architecture & Technology, Xi'an 710055, China

²College of Civil Engineering, Xi'an University of Architecture & Technology, Xi'an 710055, China

³Structure and Seismic Key Laboratory, Xi'an University of Architecture & Technology, Xi'an 710055, China

(Received September 9, 2019, Revised November 8, 2019, Accepted November 15, 2019)

Abstract. The seismic behaviour of reinforced concrete (RC) columns made from high-strength materials was investigated experimentally. Six high-strength concrete specimen columns (1:4 scale), which included three with high-strength stirrups (HSSs) and three with normal-strength stirrups (NSSs), were tested under a combination of high axial and reversed cyclic loads. The effects of stirrup strength and the ratio of transverse reinforcement on the cracking patterns, hysteretic response, strength, stiffness, ductility, energy dissipation and strain of transverse reinforcement were studied. The results indicate that good seismic behaviour of an RC column subjected to high axial compression can be obtained by using a well-shaped stirrup. Stirrup strength had little effect on the lateral bearing capacity. However, the ductility was significantly modified by improving the stirrup strength. When loaded with a large lateral displacement, the strength reduction of NSS specimens was more severe than that of those with HSSs, and increasing the stirrup strength had little effect on the stiffness reduction. The ductility and energy dissipation of specimens with HSSs were superior to those with NSSs. When the ultimate displacement was reached, the core concrete could be effectively restrained by HSSs.

Keywords: RC column; high-strength stirrups; seismic behaviour; high compression ratio; ductility

1. Introduction

Recently, the use of high-strength materials is increasing as the construction of large and high-rise structures increases. However, the brittleness of high-strength concrete becomes more obvious with an increase in concrete strength, resulting in a negative impact on the ductility and energy-absorbing ability of the structure. Therefore, an urgent problem to be solved in the engineering field is how to improve the ductility and energy dissipation of high-strength concrete.

Reinforcing concrete with stirrups can effectively improve the mechanical properties of the concrete. However, normal-strength stirrups (NSSs) prematurely yield as a result of the low yield strength and cannot provide sufficient constraint force to the core concrete. Some scholars (Guan and Guan 1999, Xiao *et al.* 2002, Yan *et al.* 2006, Shi *et al.* 2011, Thomsen and Wallace 1994, Murat and Razvi 1998, Murat and Baingo 1999, Paultre *et al.* 2001, Suzuki *et al.* 2004 among many others) have researched the use of high-strength steel bars as stirrups to improve the mechanical behaviour of high-strength

concrete. Bhayusukma and Tsai (2014) and Paultre *et al.* (2001) conducted experimental studies on the seismic behaviour of high-strength concrete columns laterally reinforced with high-strength steel bars, and the results demonstrated that a high-strength stirrup was quite effective in improving the ductility of high-strength concrete columns. The axial compression mechanical behaviour of reactive power concrete (RPC) circular columns with a spiral HSC were tested by Chen *et al.* (2017). The results indicate that the peak stress and ductility of specimens with the large stirrup ratio are increased; the high-strength spiral stirrups do not yield at the peak axial load, so the remaining strength can be ensured by the good ductility of the RPC specimens before reaching the ultimate failure status. A series of tests on the behaviour of 12 geometrically similar moderate high-strength RC columns with two different stirrups ratios was conducted under small-eccentric compression by Liu *et al.* (2018). The test results indicate that the presence of stirrups improves the strength of the specimens and makes the columns less brittle. Zheng *et al.* (2018) conducted experimental studies on the mechanical behaviour of circular concrete columns confined by high-strength spiral stirrups. The results show that the specimens with low stirrup ratios undergo single-folded shear failure, while the specimens with high stirrup ratios fail in a drum-shaped pattern. Ten cross-shaped column specimens made from high-performance concrete and high-strength stirrups (HSSs) were tested under axial compressive loading by Li *et al.* (2018). The test results show that the HSSs improve the axial compressive bearing capacity and ductility. Lee *et al.* (2017) analysed the shear behaviour of prestressed concrete members with HSSs by finite element analysis simulation. The results indicate that although the yield strength of transverse reinforcement increased the shear

*Corresponding author, Ph.D.

E-mail: wangpeng@xauat.edu.cn

^aPh.D.

E-mail: shiqx@xauat.edu.cn

^bPh.D. Student

E-mail: wangfeng900211@163.com

^cPh.D.

E-mail: wqw0815@sina.com

strength of prestressed concrete members, there was a limit to the increase in strength because of the change in shear failure modes. The seismic performance of four short concrete columns was investigated under low cycle and repeated loads by Ding *et al.* (2017). Test results reveal that the restriction effect of stirrups can improve the peak stress and the bearing capacity of the specimens can be improved. An experimental study on the seismic behaviour of short concrete columns with HSSs was conducted by the authors of the previous study (Wang *et al.* (2015)). The test results indicate that specimens with high-strength transverse reinforcement exhibited better seismic performance than those with normal-strength transverse reinforcement. Through experimental research and theoretical analysis, stress-strain behaviour of high-strength concrete confined by ultra-high-and high-strength ties was proposed by Li *et al.* (2001) and Shi *et al.* (2013a, b).

The research above mainly focuses on the mechanical behaviour and shear performance of short concrete columns with HSSs under axial compression or reversed cyclic load. However, there is still limited understanding of the seismic behaviour of long concrete columns with HSSs subjected to a reversed cyclic load. The effect of high-strength hoops on the seismic performance of long concrete columns is still far from being well understood. Therefore, there is a need to investigate and clarify the seismic behaviour of long concrete columns with HSSs.

In this paper, an experimental programme was carried out on six long, high-strength concrete columns under a combination of high axial load and reversed cyclic load, and a new-type form of stirrups is presented. The yield strength and ratio of transverse reinforcement were chosen as the design parameters. The seismic performance of the specimens was discussed in terms of crack pattern, hysteresis response, strength, stiffness, ductility, energy dissipation and strain of stirrups.

2. Experimental programme

2.1 Specimen design

Six 1/4-scale high-strength concrete columns with deformed longitudinal reinforcing bars, which included three columns with HSSs and three with normal-strength lateral reinforcement, were fabricated and tested under a combination of high axial load and reversed cyclic load; details of the specimens are shown in Fig. 1 and Table 1. The yield strength and ratio of stirrups were chosen as the test parameters in this study. The specimen columns were designed to fail in flexure failure. All columns were designed to have the same cross section of 250 mm×250 mm, and the overall specimen length was set to 1200 mm. The test specimens were cast vertically using fine aggregate commercial concrete, and the cubic concrete compressive strength measured on the 28th day was 59.27 MPa. The longitudinal reinforcement ratio was of 2.17%, which was designed according to Chinese Code (2010). Grade HRB400 steel bars were used as the longitudinal steel bars with a designed yield strength of 360 MPa. The transverse reinforcement, which was composed of normal-strength steel bars and high-strength steel bars with 135° hooks

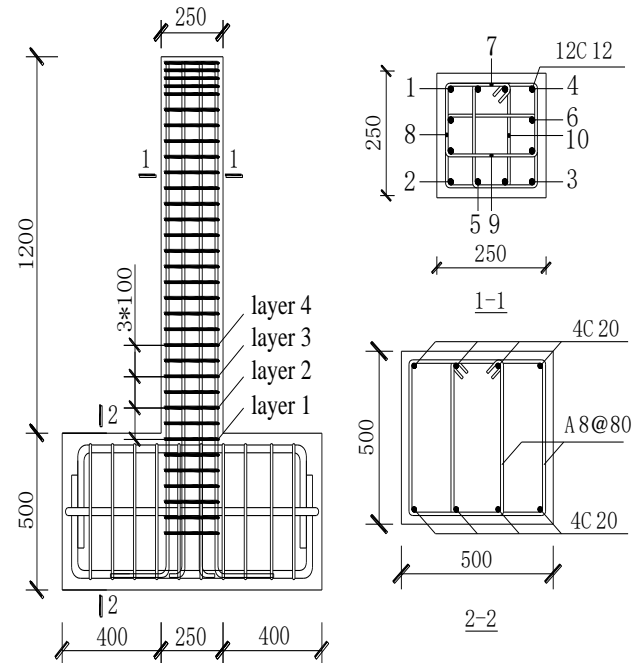


Fig. 1 Specimen dimensions and stirrup configuration

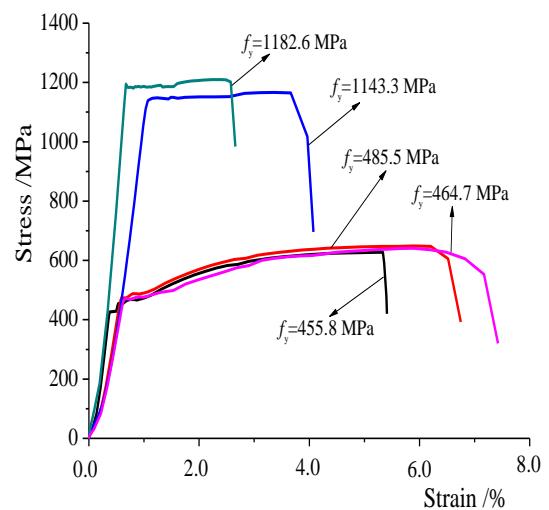


Fig. 2 Stress-strain relationship

extending with a length of 8 times the bar diameter, were used in specimens. The transverse reinforcement consisted of two normal-strength steel bars with diameters of 6 mm and 8 mm and two high-strength steel bars with diameters of 5 mm and 7 mm. The properties of the steel bars are tabulated in Table 2, and the stress-strain relationships of the steel bars are depicted in Fig. 2. A well-shaped stirrup, as shown in Fig. 1, was used in all of the column specimens to prevent the stirrup from decoupling during loading.

2.2 Instrumentation

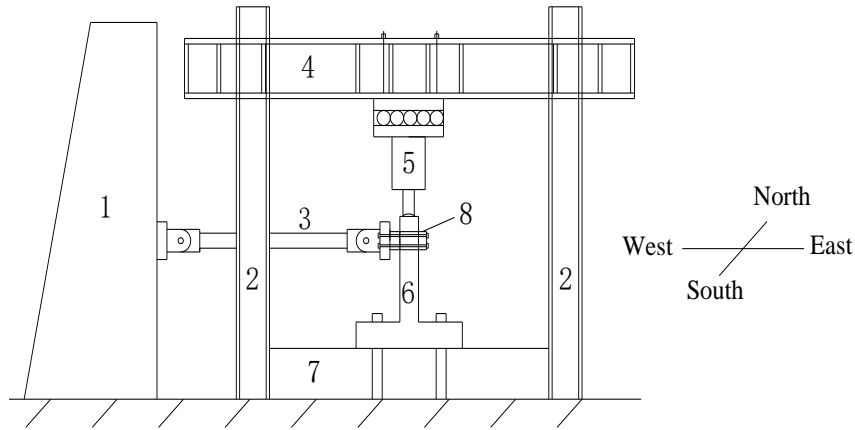
The specimens were extensively equipped with both internal and external measuring devices. Lateral displacement was measured by two horizontal displacement meters parallel to the horizontal actuator, which were mounted at the top and bottom ends of the specimens.

Table 1 Design parameters of specimens

Specimen	Axial compression ratio / axial load (kN)	Stirrups				Longitudinal steel bars		
		Strength (MPa)	Diameter (mm)	Stirrup spacing (mm)	Stirrup ratio ρ_s (%)	Number of steel bars	Diameter (mm)	Longitudinal steel bars ratio (%)
YNC-1	0.5/1358	400	8	100	1.83	12	12	2.36
YHC-1	0.5/1358	1100	7	80	1.75	12	12	2.36
YNC-2	0.5/1358	400	8	80	2.28	12	12	2.36
YHC-2	0.5/1358	1100	7	60	2.33	12	12	2.36
YNC-3	0.5/1358	400	6	60	1.71	12	12	2.36
YHC-3	0.5/1358	1100	5	42	1.70	12	12	2.36

Table 2 Properties of steel bars

Species of steel bars	Diameter /mm	Yield strength f_y /MPa	Ultimate strength f_u /MPa	Elongation δ_{10} (%)	Elastic modulus $E_s/10^5$ MPa	Shape
HRB400	5.9	455.8	639.4	18.26	2.0	Smooth
	8.0	485.5	650.4	23.83	2.0	Ribbed
	12.0	464.7	628.4	26.41	2.0	Ribbed
High-strength steel bars	4.95	1182.6	1203.4	10.2	2.0	Smooth
	7.0	1143.3	1167.2	9.14	2.0	Ribbed



1. reaction wall 2. reaction steel frame 3. 500 kN horizontal actuator 4. reaction girder 5. 2000 kN vertical actuator 6. specimen 7. test platform 8. connection braces

Fig. 3 Test setup

Strain gauges were mounted to capture the strain history in both longitudinal reinforcing bars and transverse reinforcement at critical positions, as shown in Fig. 1, where the numbers in 1-1 are the number of strain gauges. All the data were collected by a TDS-530 static data acquisition instrument.

2.3 Test setup and loading regimes

The specimens were tested at the structure and seismic key laboratory of Xi'an University of Architecture and Technology. The test setup is shown in Fig. 3. Loading was controlled by force for the initial loading cycles until the specimens were observed to start to yield. This observation was accomplished by monitoring the reaction forces of the MTS horizontal actuator. Before the horizontal low-cycle reversed load was performed, a presetting vertical load was applied on the top end of the columns, and the vertical load was constant during late loading. For the force control stage, from 50 kN, every load level was increased by 50 kN

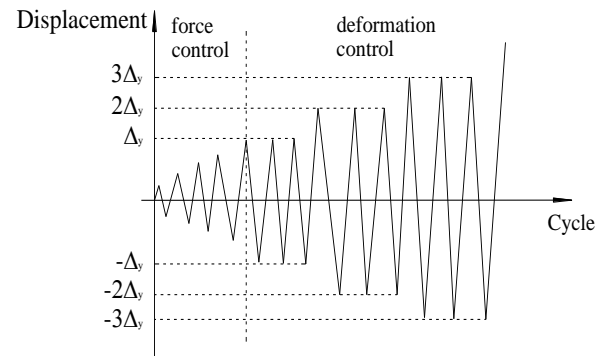


Fig. 4 Loading regime

and circulated for 1 cycle. When the specimen was observed to start to yield, the loading sequence was converted to displacement control. On the basis of the yield displacement (Δ_y), the target displacements for the cyclic loading were set as multiples of Δ_y ; the cyclic loadings were repeated three times at each target displacement level and

stopped until the reaction force decreased to approximately 50% of the maximum lateral capacity. The loading regime is shown in Fig. 4.

3. Cracking pattern

Because they had the same shear span ratio, the specimens were similar in the failure process and failure mode. The only differences were the speed of crack development and the lateral bearing capacity after maximum loading of the specimens. The final failure modes of specimens are shown in Fig. 5; a plastic hinge was formed near the bottom region of specimens during loading. However, there was no significant diagonal shear crack on columns at the end of the test. Thus, it is clear that failure mode of specimens should be classified as a flexural failure. Damage process of the specimens can be mostly divided into the following two phases.

The first loading phase is one of load-control mode. At the beginning of loading, the specimens were elastic, and the hysteresis curves almost coincided as a straight line. Under a lateral load of 120 kN, horizontal cracks occurred on the east and west sides 250 mm away from the bottom end of specimens as well as at the edge of the bottom end on another two sides. Under a lateral load of 140 kN-160 kN, horizontal cracks on the east and west sides of specimens developed throughout the cross section and a few new horizontal cracks occurred. Horizontal cracks on the south and north sides developed towards the centre of the specimens. Furthermore, vertical cracks started to occur at the corner of the bottom end of the specimens. When loaded to the yield strength of the specimens, the loading sequence was converted to displacement control mode.

Then, the specimens were subjected to the second loading phase. When loaded to $1\Delta_y$ (Δ_y is the yield displacement), penetrating cracks increased gradually on both the east and west sides of the bottom end of the specimen. Cracks on the south and north sides gradually developed towards the centre of the specimens. Cracks occurred intensively at the corner of the specimens and developed along the height of the specimens. When loaded to $2\Delta_y$, crack development tended to be stable, and the corner concrete and cover concrete of the east and west sides started to spall. When loaded to $3\Delta_y$, the width of the original horizontal and vertical cracks increased. The concrete at the bottom end of specimens was crushed. When loaded to $4\Delta_y$, concrete at the bottom end was crushed and spalled. The maximum width of the cracks reached 1 mm on the east and west sides, and the longitudinal steel bars began to yield. When loaded to $5\Delta_y$ - $6\Delta_y$, no new cracks developed; the cover concrete was crushed and dropped seriously. Finally, the specimens failed at a displacement of $7\Delta_y$ - $8\Delta_y$. The longitudinal steel bars and stirrups were exposed at the bottom end of the column. The core concrete of the HSSs specimens was not crushed, while crush of the core concrete was observed for the specimens with NSSs. It implies that HSSs can improve the constraint effect of core concrete; hence, they can modify the seismic behaviour of high-strength concrete columns.

4. Test result analysis

4.1 Hysteresis characteristics

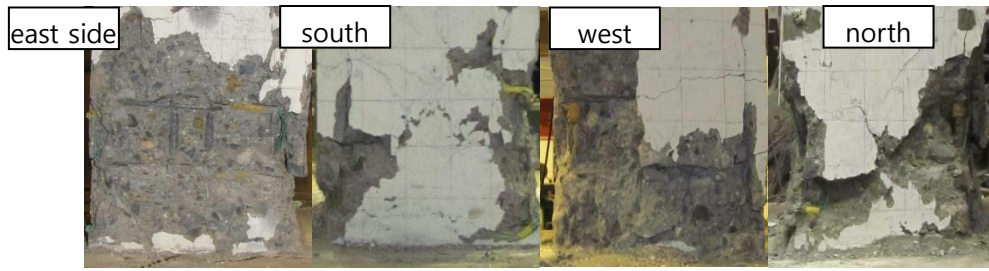
The hysteresis curves can comprehensively reflect the relationship between the load and the deformation of the member. Hysteresis curves obtained from the test are shown in Fig. 6. In both the NSS specimens and HSS specimens, the hysteresis characteristics have the following features in common. Before the specimens reach their yield load, the hysteresis curves are narrow with small energy dissipation, and stiffness degradation is not obvious. However, after yielding, energy dissipation capacity is improved with an increasing area of hysteresis loops. While at the same target displacement, the lateral bearing capacity and stiffness of the last two cycles were lower than those of the first cycle. After the maximum lateral bearing capacity, shear bearing capacity and stiffness started to reduce as a result of cover concrete spall. Fig. 6 also indicates that the stirrup strength and stirrup ratio significantly affect the hysteresis loops. Under the condition of a similar hoop ratio, the load cycle number of the HSS specimen is obviously greater than that of the NSS specimen, and the hysteresis curve is plump. After the maximum load, the strength decays slowly and the deformation ability is large. Even when the ultimate displacement is reached, the hysteresis curve is still stable and the bearing capacity does not suddenly drop. However, the NSS specimen is characterized by few load cycles, rapid strength reduction, poor deformability, small ultimate displacement, and poor energy dissipation. Therefore, the use of high-strength composite stirrups to restrain high-strength concrete columns is an effective measure to improve the ductility of high-strength concrete columns under high axial compression.

4.2 Skeleton curves

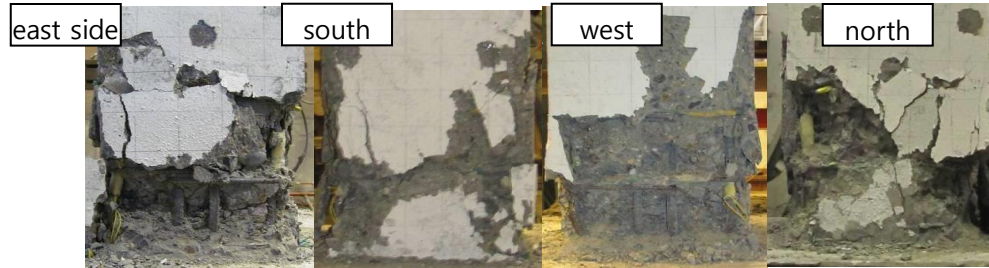
Skeleton curves can reflect many characteristics, such as yield load, maximum load and ductility. Skeleton curves obtained from the test are shown in Fig. 7. The results show that increasing the stirrup strength has little effect on the horizontal bearing capacity of the specimen. However, the ductility is significantly improved by increasing the stirrup strength. Due to the restraining effect of HSSs, the skeleton curve of the specimen decreases gently under a high axial compression ratio, and there is no steep drop. The deformation and ductility of RC columns with HSSs are better than those of columns confined with normal-strength hoops.

4.3 Strength and stiffness

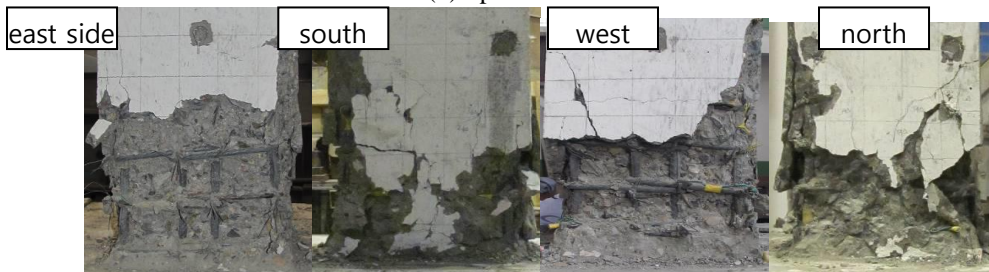
Under low-cycle repeated loading, the bearing capacity of the specimen will decrease with an increase in the number of loading cycles under a certain displacement. This phenomenon is called strength reduction. The strength reduction of structural members has a great influence on its mechanical properties, and the faster the strength decays, the faster the ability of the structure to resist loads is reduced.



(a) Specimen YHC-1



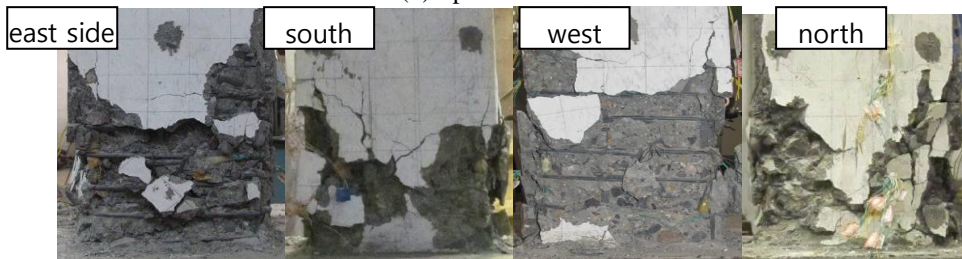
(b) Specimen YNC-1



(c) Specimen YHC-2



(d) Specimen YNC-2



(e) Specimen YHC-3



(f) Specimen YNC-3

Fig. 5 Failure mode

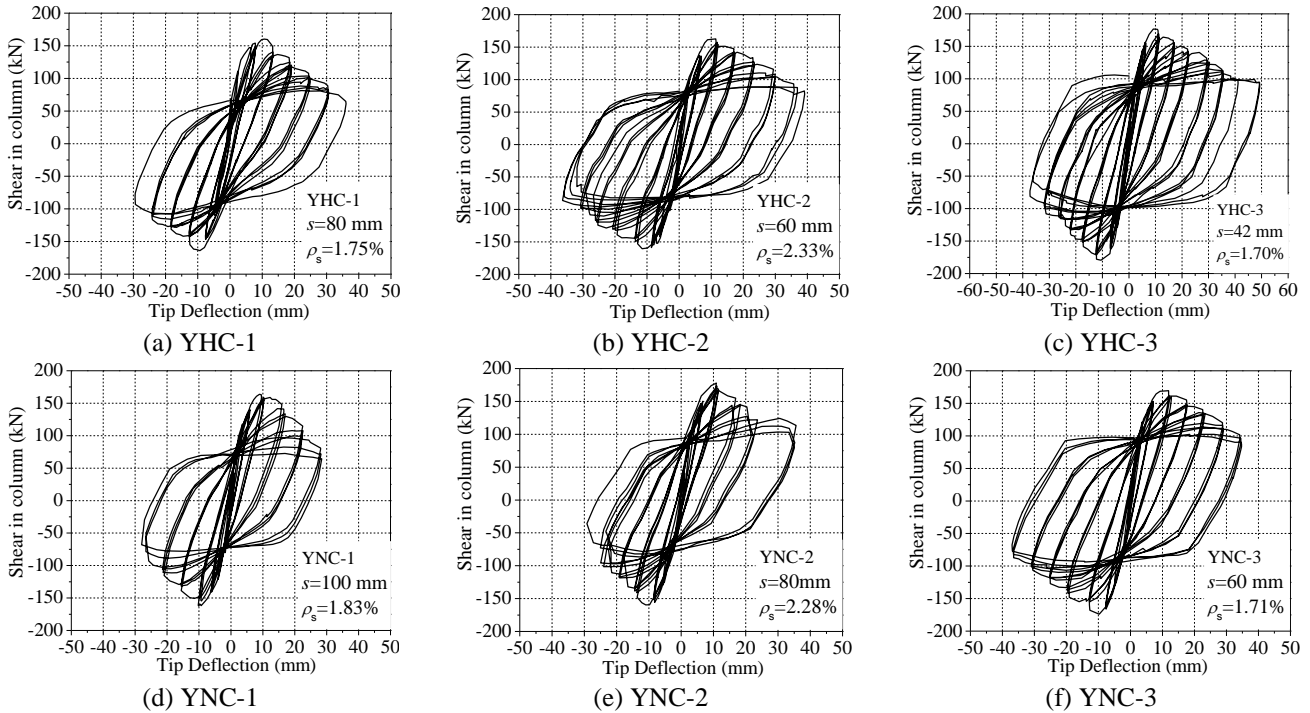


Fig. 6 Hysteresis curves of specimens

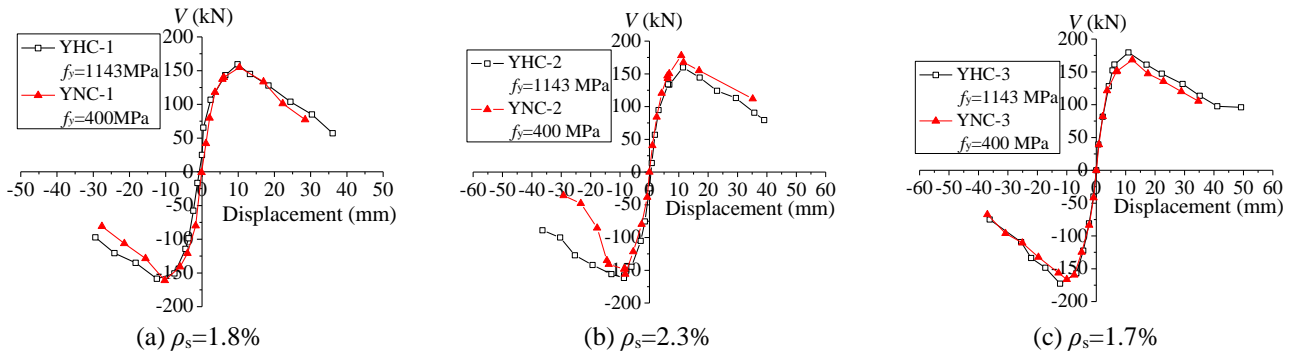


Fig. 7 Skeleton curves

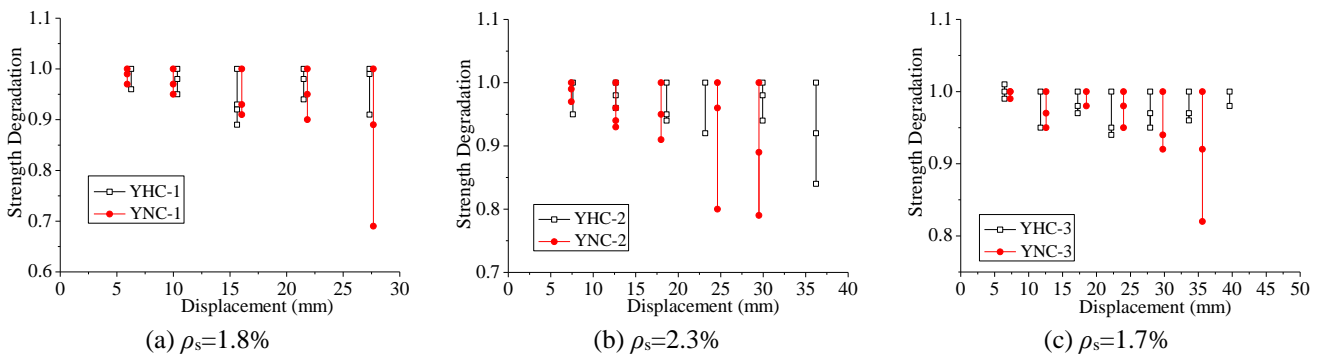


Fig. 8 Effect of stirrup strength on strength reduction

Strength reduction is represented by the ratio V_n/V_1 of the maximum load of the n^{th} cycle under a certain displacement level to the maximum load at the 1st cycle. Fig. 8 depicts the influence of stirrup strength on the strength reduction of a specimen under the same hoop ratio. It is seen that the stirrup strength has little effect on the strength reduction of a specimen under a small lateral

displacement, while it affects the strength reduction of a specimen subjected to a large lateral displacement. When loaded to a large lateral displacement, the strength reduction of the NSS specimen is more severe than that of the high-strength hoop specimen. This is mainly because the constraints of the stirrups on the concrete are passive constraints. The larger the transverse deformation of the

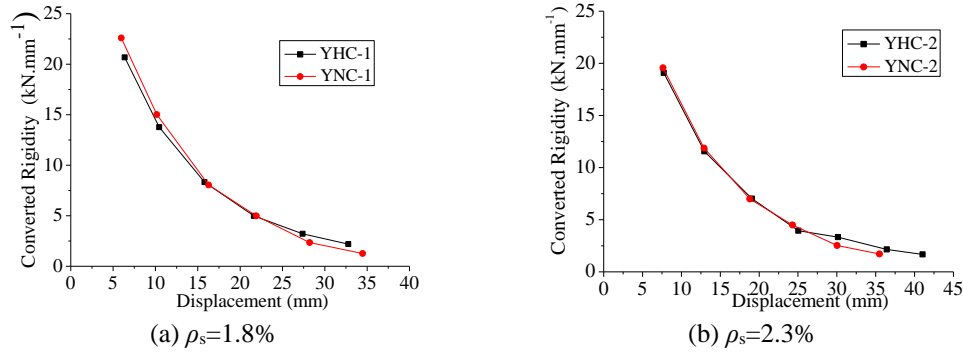


Fig. 9 Stiffness reduction

Table 3 Lateral force, displacement, ductility coefficient and ultimate drift ratio

Specimen	Cracking		Yielding		Maximum		Ultimate		μ_{Δ}	θ_p
	Force/kN	Dis./mm	Force/kN	Dis./mm	Force/kN	Dis./mm	Force/kN	Dis./mm		
YHC-1	82	2.42	126	4.57	159	9.86	135	16.12	3.53	1/52
	-124	-3.71	-136	-6.21	-159	-12.44	-135	-18.36	2.96	-1/46
YNC-1	118	3.61	135	5.42	154	10.36	132	17.30	3.19	1/49
	-129	-4.77	-137	-5.61	-161	-10.25	-137	-14.20	2.52	-1/60
YHC-2	120	3.13	136	7.35	160	11.45	136	19.67	2.68	1/43
	-80	-2.94	-129	-4.87	-161	-8.65	-137	-21.21	4.36	-1/40
YNC-2	120	4.21	156	7.53	178	10.88	151	18.53	2.46	1/46
	-122	-5.5	-131	-6.28	-156	-8.22	-132	-14.63	2.33	-1/58
YHC-3	128	4.27	153	5.61	180	10.97	153	20.27	3.62	1/42
	-122	-4.4	-146	-6.04	-173	-12.26	-147	-17.78	2.94	-1/47
YNC-3	121	3.67	137	5.38	168	12.25	143	19.4	3.61	1/44
	-125	-4.92	-141	-6.13	-166	-10.00	-141	-17.10	2.79	-1/50

specimen is, the more obvious the restraining effect of the stirrup on the core concrete; the high-strength stirrup has a large yield strength and strong constraint on the core concrete, which can slow the rate of strength reduction of the specimen under large deformation.

As the lateral displacement and the number of loading cycles increase, the stiffness of the member will also decrease. The secant stiffness, which is used to describe the stiffness of the member, can be calculated as follows

$$K_i = P_i / \Delta_i \quad (1)$$

where K_i is the secant stiffness of the i^{th} loading cycle, P_i is the horizontal load corresponding to the maximum displacement of the i^{th} loading cycle, and Δ_i is the maximum displacement of the i^{th} loading cycle. Fig. 9 gives the secant stiffness versus displacement for some of the specimens in this test. It can be seen that in the initial stage of loading, the stiffness of the specimen decreases rapidly and then gradually decreases with increased displacement; the stirrup strength has little effect on the stiffness reduction. This is mainly because the stiffness of the specimen is primarily composed of concrete and longitudinal steel bars, while the stirrups contribute little to the stiffness.

4.4 Ductility

Ductility illustrates the deformation capacity of a

structural component after reaching the maximum lateral capacity. In this paper, the ductility coefficient and ultimate drift ratio were taken to describe the deformation capacity of the specimens. The computational expressions are as follows

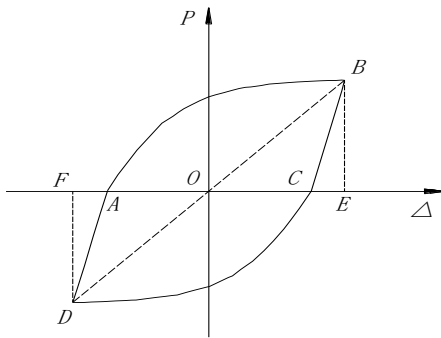
$$\mu_{\Delta} = \Delta_u / \Delta_y \quad (1)$$

$$\theta_p = \Delta_u / H \quad (2)$$

where μ_{Δ} is the ductility coefficient, θ_p is the ultimate drift ratio, Δ_u is the ultimate displacement, Δ_y is the yield displacement, and H is the clear length of the specimen. The yield displacement is determined by the equal energy method. The ultimate displacement is that at which 80% of the peak lateral load is sustained, and the corresponding lateral load is defined as the ultimate load. Thus, the load, displacement, ductility coefficient and ultimate drift ratio of specimens under various loading status are shown in Table 3 (positive values and negative values represent the force or displacement (dis.) in the push and pull directions, respectively). It can be seen that the ductility coefficient of concrete columns with HSSs is larger than 3, and the ultimate drift ratio is larger than 1/50, which shows good ductility and strong anti-collapse ability. For NSS specimens YNC-1 and YNC-2, the ductility coefficients are 2.86 and 2.40, respectively, and the ductility is poor. At the same time, their ultimate drift ratios are 1/54 and 1/51, both less than 1/50, which is the requirement of the Chinese

Table 4 Energy dissipation of RC columns

Dis. level	YHC-1		YNC-1		YHC-2		YNC-2		YHC-3		YNC-3	
	Cycling times	Energy kN·mm										
1 Δ_y	3	2506	3	1335	3	1840	3	1738	3	1462	3	1681
2 Δ_y	3	4768	3	3553	3	5757	3	7067	3	5175	3	5564
3 Δ_y	3	10786	3	8630	3	10054	3	9962	3	10251	3	11029
4 Δ_y	3	13649	3	12950	3	15848	3	14732	3	14582	3	14948
5 Δ_y	3	19423	3	19481	3	21573	3	20831	3	20797	3	23114
6 Δ_y	1	9501	1	8916	3	28720	1	9356	3	27138	3	31113
7 Δ_y					1	11115			3	34291	1	13153
8 Δ_y									1	14383		
Gross		60633		54865		94907		63686		128079		100602

Fig. 10 The calculation diagram of h_e

earthquake-resistance specifications (GB 50011-2010 (2010)). Furthermore, specimen YNC-3 with a hoop ratio of 1.71% has a larger ductility coefficient and ultimate drift ratio than specimen YNC-2 with a hoop ratio of 2.28% does. This indicates that reducing stirrup spacing is an effective method to improve the seismic performance of the RC columns. The maximum lateral capacity of the specimens YHC-1 and YNC-2 are comparable, but specimen YHC-1 with HSSs requires 30% less steel.

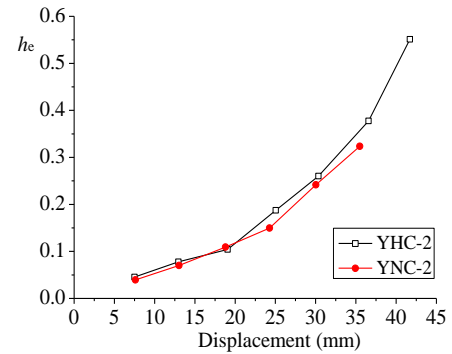
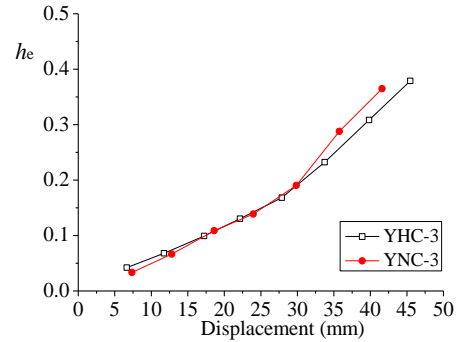
4.5 Energy dissipation capacity

In this paper, two indexes are used to reflect the energy dissipation capacity of the specimens. One index is the equivalent viscous damping coefficient h_e , and the other index is cumulative energy dissipation. Analysing the hysteresis loops allows the degree of energy dissipation under different loading levels to be investigated. The calculation formula of the h_e can be written as follows

$$h_e = S_{(ABCD A)} / (2\pi \cdot S_{(OBE+ODF)}) \quad (4)$$

where $S_{(ABCD A)}$ represents the area of hysteresis loop ABCDA and $S_{(OBE+ODF)}$ represents the area of triangles OBE and ODF, as depicted in Fig. 10.

The equivalent viscous damping coefficients of the test specimen are shown in Fig. 11, where the results are calculated based on the last hysteresis loop at every target displacement. It can be seen that under the same stirrup ratio, the h_e of columns with HSSs is close to that of columns with NSSs at the beginning of loading. However, in late loading under a good condition of constraints

(a) $\rho_s=2.3\%$ (b) $\rho_s=1.7\%$ Fig. 11 h_e of specimens

($\rho_s=2.3\%$), the h_e of columns with HSSs is significantly larger than that of columns with NSSs, and the columns also exhibit a large damage displacement. The effect of the stirrup strength on the h_e of specimens under the same stirrup spacing is depicted in Fig. 12. It is seen that under the same stirrup spacing, the h_e of HSS column YHC-1 is larger than that of NSS column YNC-2. Since a high-strength tie specimen has a low stirrup ratio, the required number of stirrups is low. Therefore, to achieve the same energy dissipation, columns adopting HSSs can use less steel than those using normal-strength ties. Under a high axial compression ratio, HSS column YHC-2 can possess an equivalent viscous damping coefficient as high as 0.55, so by using high-strength reinforcing steel bars instead of normal-strength reinforcing steel bars as transverse reinforcement, the seismic behaviour of the RC column can be effectively improved.

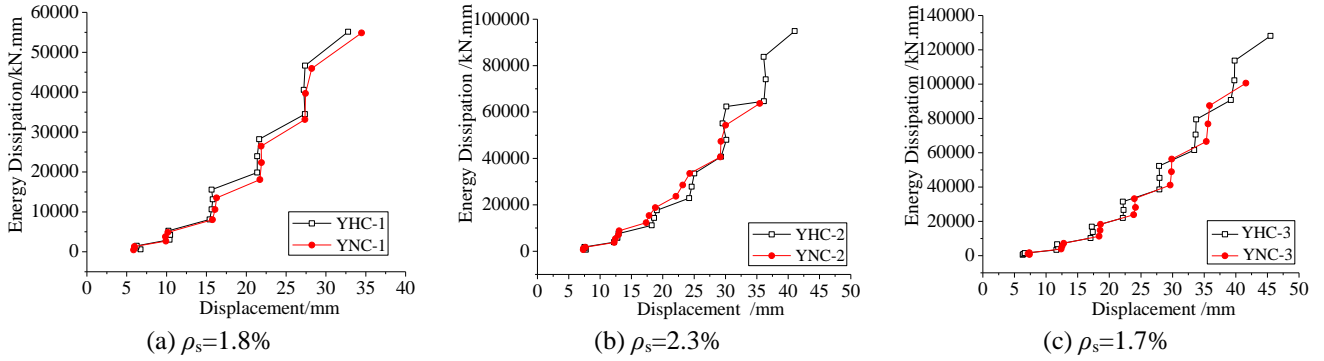


Fig. 13 Effect of stirrup strength on cumulative energy dissipation

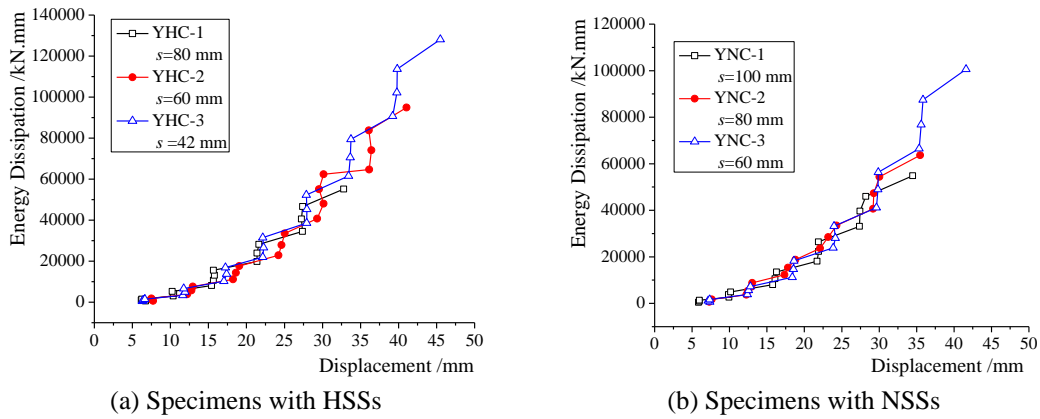


Fig. 14 Effect of stirrup spacing on cumulative energy dissipation

The cumulative energy dissipation (CED) of test specimens is the area of all the hysteresis loops. The calculation formula of CED can be written as follows

$$E_x = \int P(x)dx \quad (5)$$

where $P(x)$ represents the formula of hysteresis loops. At each displacement level, the energy dissipation of the specimens is tabulated in Table 4, and the values of CED against the lateral displacement are depicted in Fig. 13. Due to less energy dissipation before the specimen yields, this part of the energy dissipation is neglected when calculating the CED. After the specimen yields, the CED increases with an increased number of loading cycles. Compared with columns confined with normal-strength ties, the CED of columns with HSSs is significantly improved. When loaded to ultimate displacement, the CED values of the high-strength hoop columns had stirrup ratios of 1.7%, 1.8% and 2.3%, which are 27.3%, 10.5% and 49.0% larger than those of the normal-strength hoop columns, respectively. This finding demonstrates that HSSs can significantly improve the energy dissipation of components.

To investigate the effect of stirrup spacing on CED, the cumulative energy dissipation against stirrup spacing is shown in Fig. 14. Specimens YHC-3 and YNC-3 with a low stirrup ratio of 1.7% possess the strongest energy dissipation among the high- and normal-strength hoop specimens. Thus, when the stirrup spacing is made smaller, even at a small hoop ratio, the concrete column can also obtain better energy dissipation performance.

4.6 Stirrup strain

It is important to investigate the stress level of stirrups in RC columns since it can reflect the confinement status of the core concrete. The relationship of stirrup strain versus is shown in Fig. 15, where the horizontal line represents the yielding strain of the stirrup, and the two vertical lines represent the drift corresponding to the maximum lateral force and ultimate lateral force. It can be seen that when loaded to the maximum lateral capacity of the specimen, the strain of the stirrups is within 0.002 (the corresponding stress is 400 MPa) and in a low-stress state for HSSs, while it is in a high-stress state for NSSs. Then, with an increase in drift, the stirrup strains increase rapidly. When loaded to a drift of approximately 1/50 (2.0%), most of the NSS specimens have reached or nearly reached the yield strength, and the core concrete could not be confined effectively. At this time, the concrete in the plastic hinge area is mostly crushed under repeated horizontal loads, and the specimens promptly fail. By contrast, the HSSs are far from the yield strength. The core concrete can still be confined effectively by HSSs. However, the cover concrete has been seriously peeled off and the bearing capacity of the specimen fell to 85% of the maximum load and reached the limit state. It can be seen that the NSSs have reached, or almost reached, the yielding strength; hence, it could not form an effective constraint on the core concrete. The strength advantage of HSSs can ensure that the stirrup does not yield before the failure of the member, and the core concrete can be effectively restrained by stirrups. Therefore,

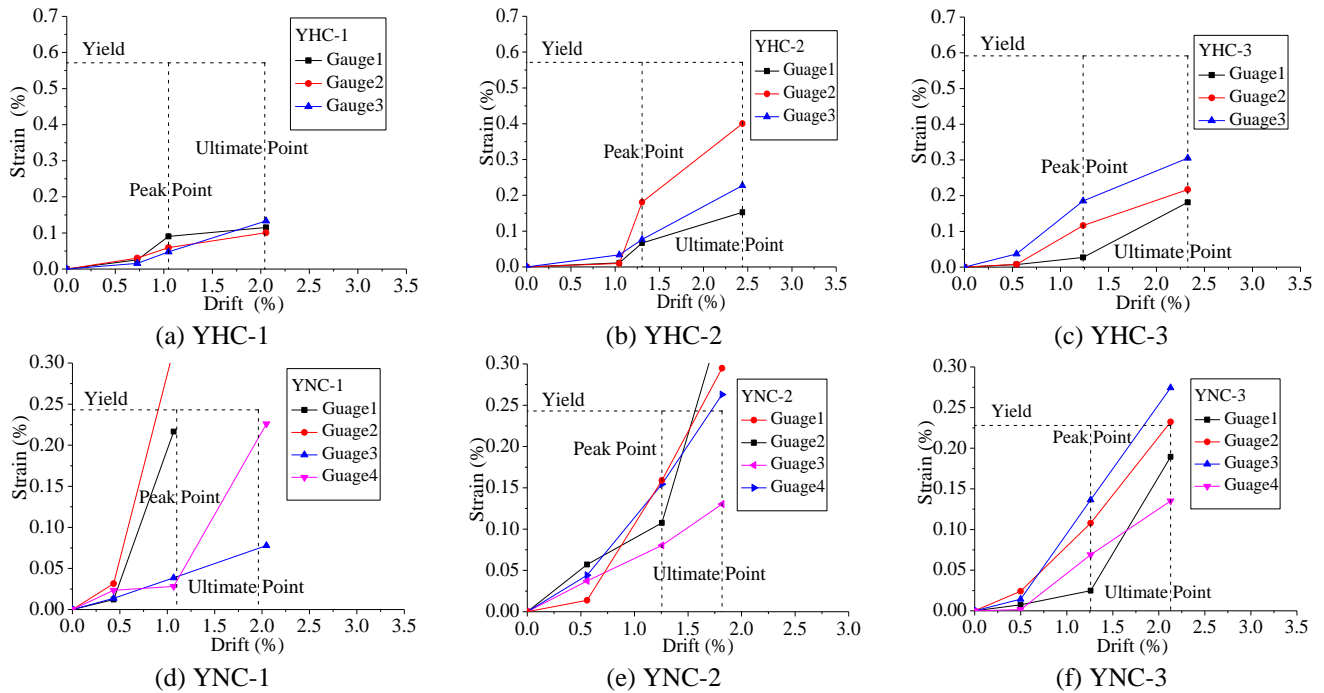


Fig. 15 Specimen stirrup strain (Note: the strain value in Fig. 15 is the maximum strain value of the gauge readings in the same layer)

seismic performance of the specimens is increased.

5. Conclusions

An experimental programme was carried out on six high-strength concrete columns under high axial compression and low cyclic reversed loading. The performance of specimens was discussed in terms of cracking and failure pattern, hysteretic response, ductility, strength reduction, energy dissipation and strain of transverse reinforcement. The following conclusions can be drawn.

- Under a high axial compression ratio, good ductility and energy dissipation capacity of the HSS or NSS specimens can be obtained by using a well-shaped stirrup.
- Stirrup strength has little effect on the lateral bearing capacity. However, the ductility was significantly modified by improving stirrup strength. Reducing stirrup spacing is an efficient method to improve the seismic behaviour of the columns.
- Stirrup strength has little effect on the strength reduction of a specimen under a small lateral displacement, while it significantly affects the strength reduction of a specimen subjected to a large lateral displacement. When loaded to a large lateral displacement, the strength reduction of the NSS specimen is more severe than that of the HSS specimen, and increasing the stirrup strength has little effect on the stiffness reduction.
- The ductility and energy dissipation of specimens with HSSs are superior to those with NSSs. The ductility of specimens YHC-1, YHC-2 and YHC-3 is increased by

11.9%, 39.6% and 3.15%, respectively. The energy dissipation of specimens YHC-1, YHC-2 and YHC-3 is increased by 10.2%, 49% and 27.3%, respectively.

- When loaded to the maximum lateral capacity of the specimens, the strains of NSSs are almost in the yielding state, while the HSSs are still in the low-stress working condition due to its greater strength. When the ultimate displacement is reached, the HSSs do not yield and the core concrete can be effectively restrained by stirrups. Therefore, the specimen with HSSs has good bearing capacity and ductility and shows good anti-collapse ability.

Acknowledgements

The authors would like to thank the National Key Research and Development Program (NO. 2017YFC0703406), the National Natural Sciences Foundation of China (NO. 51608434, NO. 51878543 and NO. 51878540) and the Independent Research and Development project of State Key Laboratory of Green Building in Western China (NO. LSZZ202018) for their generous financial support of the project.

References

- Bhayusukma, M.Y. and Tsai, K.C. (2014), "High-strength RC columns subjected to high-axial and increasing cyclic lateral loads", *Earthq. Struct.*, 7(5), 779-796. <https://doi.org/10.12989/eas.2014.7.5.779>.
- Chen, M., Zheng, W. and Hou, X. (2017), "Experimental study on mechanical behavior of RPC circular columns confined by high-strength stirrups under axial compression", *Funct. Mater.* 24(1),

- 82-90. <https://doi.org/10.15407/fm24.01.082>.
- Ding, H.Y., Liu, Y., Han, C. and Guo, Y.H. (2017), "Seismic performance of high-strength short concrete column with high-strength stirrups constraints", *Tran. Tianjin U.*, **23**, 360-369. <https://doi.org/10.1007/s12209-017-0059-9>.
- GB 50011-2010 (2010), *Code for Seismic Design of Buildings*, Beijing, China.
- Guan, P. and Guan, Q. (1999), "Effect of cold-rolled ribbed wires hoping on ductility of high-strength concrete columns", *J. Dalian Univ.*, **20**(4), 56-58. <https://doi.org/10.1999.04.014>.
- Lee, J.Y., Lim, H.S. and Kim, S.E. (2017), "Evaluation of applicability of high strength stirrup for prestressed concrete members", *Int. J. Struct. Constr. Eng.*, **11**(6), 718-723. <https://doi.waset.org/Publication/10007191>.
- Li, B., Park, R. and Tanaka, H. (2001), "Stress-strain behavior of high-strength concrete confined by ultra-high-and normal-strength transverse reinforcement", *ACI Struct. J.*, **98**(3), 395-406. <https://doi.org/10.14359/10228>.
- Li, W., Sun, L., Yang, F. and Yang, K. (2018), "Axial compressive behaviour of special-shaped steel-fibre-reinforced concrete columns", *Struct. Build.*, **5**, 1-17. <https://doi.org/10.1680/jstbu.17.00118>.
- Liu, J., Zixing, D., Dong, L. and Xiuli, D. (2018), "Experimental and numerical investigations on the size effect of moderate high-strength reinforced concrete columns under small-eccentric compression", *Int. J. Dam. Mech.*, **27**, 657-685. <https://doi.org/10.1177/1056789517699054>.
- Murat, S. and Baingo, D. (1999), "Circular high-strength concrete columns under simulated seismic loading", *J. Struct. Eng.*, **125**, 272-280. [https://doi.org/10.1061/\(asce\)07339445\(1999\)125:3\(272\)](https://doi.org/10.1061/(asce)07339445(1999)125:3(272)).
- Murat, S. and Razvi, S.R. (1998), "High-strength concrete columns with square sections under concentric compression", *J. Struct. Eng.*, **124**, 1438-1447. <https://doi.org/10.14359/736>.
- Paultre, P., Legeron, F. and Mongeau, D. (2001), "Influence of concrete strength and transverse reinforcement yield strength on behavior of high-strength concrete columns", *ACI Struct. J.*, **98**, 490-501. <https://doi.org/10.14359/10292>.
- Shi, Q., Wang, N., Wang, Q. and Men, J. (2013a), "Uniaxial compressive stress-strain model for high-strength concrete confined with high-strength lateral ties", *Eng. Mech.*, **30**(5), 131-137. <https://doi.org/10.4334/jkci.2005.17.5.843>.
- Shi, Q., Yang, K., Bai, L., Zhang, X. and Jiang, W. (2013b), "Study on stress-strain relationship of high-strength concrete confined with high-strength stirrups under axial compression", *J. Build. Struct.*, **34**(5), 144-151. <https://doi.org/10.14006/j.jzjgxb.2013.04.014>.
- Shi, Q., Yang, K., Bai, L., Zhang, X. and Jiang, W. (2011), "Experiments on seismic behavior of high-strength concrete columns confined with high-strength stirrups", *China Civil Eng. J.*, **44**(12), 9-17. <https://doi.org/10.2495/amitp130101>.
- Suzuki, M., Akiyama, M., Hong, K.N., Cameron, I.D. and Wang W.L. (2004) "Stress-strain model of high-strength concrete confined by rectangularties", *Proceedings of the 13th World Conference on Earthquake Engineering*, Vancouver, British Columbia, Canada, August.
- Thomsen, J.H. and Wallace, J.W. (1994), "Lateral load behavior of reinforced concrete columns constructed using high-strength materials", *ACI Struct. J.*, **91**, 605-615. <https://doi.org/10.14359/4181>.
- Wang, P., Shi, Q., Wang, Q. and Tao, Y. (2015), "Experimental behavior and shear bearing capacity calculation of RC columns with a vertical splitting failure", *Earthq. Struct.*, **9**(6), 1233-1250. <https://doi.org/10.12989/eas.2015.9.6.1233>.
- Xiao, Y., Wu, Y., Shang, S., Henry, W.Y. and Esmaeily, A. (2002), "Experimental and analytical studies on full-scale high-strength concrete columns", *J. Southeast Univ. (Nat. Sci. Edi.)*, **32**(5), 746-749. <https://doi.org/10.3321/j.issn:1001-0505.2002.05.015>.
- Yan, S., Xiao, X., Zhang, Y. and Kan, L. (2006), "Seismic performances of square HSC columns confined with high-strength PC rebar", *J. Shenyang Jianzhu Univ. (Natural Science Edition)*, **22**(1), 7-10. <https://doi.org/10.14359/4362>.
- Zheng, W., Hou, C. and Chang, W. (2018), "Experimental study on mechanical behavior of circular concrete columns confined by high-strength spiral stirrups", *J. Build. Struct.*, **39**(6), 21-31. <https://doi.org/10.15407/fm24.01.082>.

KT

